CWE-8
June 7-11, 2026
London, ON, Canada

Wind flow field reconstruction by boundary condition identification in structures from sparse measurements.

T. Ansari[a,b], S. Warnakulasuriya[a], A. Kodakkal[a], I. Antonau[c,e], H. Antil[d], R. Löhner[d,b], R. Wüchner[a]

[a]Chair of Structural Analysis, Technical University of Munich, Munich, Germany, talhah.ansari@tum.de; suneth.warnakulasuriya@tum.de; anoop.kodakkal@tum.de; wuechner@tum.de
[b]Institute for Advanced Study, Technical University of Munich, Munich, Germany
[c]Institute of Structural Analysis, Technical University of Braunschweig, Germany, ihar.antonau@tu-braunschweig.de
[d]College of Science, George Mason University, Virginia, United States, hantil@gmu.edu; rlohner@gmu.edu
[e]Cluster of Excellence SE^{2}A – Sustainable and Energy-Efficient Aviation, Technische Universität Braunschweig

Summary

An adjoint-based methodology to identify the boundary conditions and thereby reconstruct the flow field in structures under wind flow from limited point measurements within the flow field is proposed. The identification problem is formulated as an optimization problem in which the aggregated differences between the velocity and pressure measurements and the computed values at a few sensor locations are minimized by adjusting the inlet parameters. In this exploratory study, the feasibility of this endeavour is analyzed using RANS to model fluid flow and identify the inlet velocity profile. Multiple numerical examples are analyzed to illustrate the applicability of the approach.

Keywords: *System identification, digital twin, flow field reconstruction, inlet velocity identification*

1 INTRODUCTION

Computational fluid dynamics is widely used to estimate wind effects on structures, complementing traditional wind tunnel testing and real-world testing. Accurate knowledge of the wind flow field is critical to both methods for estimating structural loads and, therefore, how the structure responds to these load scenarios. Traditional experimental methods, whether in a wind tunnel or real-world testing, limit the ability to measure wind velocity/pressure at only a fixed number of observation points. Due to the scarcity of measurements, it is challenging to reconstruct the entire flow field. Numerical methods like the RANS in CFD, together with system identification techniques, are explored in this context to explore methods to overcome the aforementioned challenges.

Inverse modelling and system identification have been explored in the past using adjoint-based parameter identification for damage localization in structures identification (Löhner et al. 2024), boundary and load identification (Ansari et al. 2025b), and thermal field reconstruction (Ansari et al. 2025a). Despite these studies, the use of adjoint-based methodologies for identifying flow conditions in wind problems remains largely unexplored. We propose and solve the inverse problem by adjoint techniques to identify the flow field from sparse (velocity and pressure) measurements from the flow field. Section 2 outlines the details of the adjoint-based methodology proposed and used for the wind flow identification. Section 3 details the numerical examples explored, and the section 4 presents the results and conclusions from the study.

2 METHODOLOGY

Let $\underline{\eta}$ be the vector of parameters to be identified. In this case, the inlet parameters (such as velocity and turbulence model parameters (k, ω, ϵ, etc) at the inlet boundary/surface). For a discretized system, consisting of a finite number of velocity and pressure sensors, this parameter identification problem can be formulated as an optimization problem with the minimization cost function:

$$J(\underline{\mathbf{u}}, \underline{p}, \underline{\eta}) = \frac{1}{2}\sum_{j_u=1}^{m_u} w_{j_u}^u (\underline{\mathbf{I}}_{j_u}^u \cdot \underline{\mathbf{u}}(\underline{\eta}) - \mathbf{u}_{j_u}^{\text{meas}})^2 + \frac{1}{2}\sum_{j_p=1}^{m_p} w_j^p (\underline{\mathbf{I}}_{j_p}^p \cdot \underline{p}(\underline{\eta}) - p_{j_p}^{\text{meas}})^2 \quad , \tag{1}$$

where $j_u = 1, m_u$ refers to the m_u measuring points of the velocity ($\boldsymbol{u}_{j_u}^{\text{meas}}$); $j_p = 1, m_p$ refers to the m_p measuring points of the pressure ($p_{j_p}^{\text{meas}}$); $\underline{\mathbf{I}}_{j_u}^u$, $\underline{\mathbf{I}}_{j_p}^p$ refer to the interpolation matrices used to obtain the model response (velocities and the pressures, respectively) at the measurement locations; and $w_{j_u}^u$, $w_{j_p}^p$ are the sensor weights for the j_u-th velocity and j_p-th pressure sensor respectively.

Since this study considers steady-state incompressible RANS with two-equation (such as $k-\epsilon$, $k-\omega$, or $k-\omega-SST$) turbulence models (Menter 1993), the equations to be considered are:

$$\begin{aligned} r^{u_i} &= u_j \frac{\partial u_i}{\partial x_j} - \frac{\partial}{\partial x_j}\left([\nu + \nu_t]\frac{\partial u_i}{\partial x_j}\right) + \frac{1}{\rho}\frac{\partial p}{\partial x_j} - g_i = 0 \quad , \quad r^p = \frac{\partial u_i}{\partial x_i} = 0 \\ r^\phi &= u_{\phi,i}\frac{\partial \phi}{\partial x_i} - \frac{\partial}{\partial x_i}\left(\nu_\phi \frac{\partial \phi}{\partial x_i}\right) + s_\phi \phi - f_\phi = 0 \end{aligned} \tag{2}$$

Eq. (2) shows the momentum equation residual (r^{u_i}) - where $u_i \in [u, v, w]$, continuity equation residual (r^p), and scalar transport equation (r^ϕ) residual used to compute the scalar turbulence quantities (ϕ can be k, ω, or ϵ depending on the RANS turbulence model), where $u_{\phi,i}$ is effective velocity, ν_ϕ is effective kinematic viscosity, s_ϕ is the reaction term, and f_ϕ is the source term.

The cost function in Eq. (1) is minimized subject to these residuals as constraints. Eqn. (2) represents the strong form of the momentum, continuity, and scalar transport equations. For FEM, their weak form (here, referred as $\underline{R}^u, \underline{R}^v, \underline{R}^w, \underline{R}^p, \underline{R}^k, \underline{R}^\epsilon, \underline{R}^\omega$) is used, which suffers from numerical instabilities, thus stabilization is preferred. In this work, the Residual-based-Flux-Corrected Stabilization method is used (Warnakulasuriya 2022). Since the primal problem uses stabilization, it is necessary to also consider the derivatives of the stabilization terms during gradient calculation. Additionally, here we shall use frozen turbuluence such that $\partial \underline{R}^{u_i}/\partial \underline{k} = \partial \underline{R}^{u_i}/\partial \underline{\omega} = \underline{0}$.

The Lagrangian and its derivative w.r.t. the design variables is shown in Eq. (3) where $\underline{R}$ contains all the residual equations described earlier and is dependant on the design variables $\underline{\eta}$ and the state variables $\underline{\lambda} = [u, v, w, p, k, \omega]^\top$. $\tilde{\underline{\lambda}}$ are the corresponding adjoint variables. Eq. (4) shows the adjoint problem to obtain $\tilde{\underline{\lambda}}$, which is used to get the gradient.

$$L = J + \tilde{\underline{\lambda}}^\top \underline{R}\left(\underline{\lambda}\left(\underline{\eta}\right), \underline{\eta}\right) \quad , \quad \frac{dL}{d\underline{\eta}}^\top = \frac{\partial J}{\partial \underline{\eta}}^\top + \tilde{\underline{\lambda}}^\top \frac{\partial \underline{R}}{\partial \underline{\eta}} + \underbrace{\left[\frac{\partial J}{\partial \underline{\lambda}}^\top + \tilde{\underline{\lambda}}^\top \frac{\partial \underline{R}}{\partial \underline{\lambda}}\right]}_{\text{adjoint problem: } \tilde{\underline{R}}^\top} \frac{d\underline{\lambda}}{d\underline{\eta}} \quad , \tag{3}$$

$$\tilde{\underline{R}}^\top = \underline{0} \implies \tilde{\underline{\lambda}}^\top \frac{\partial \underline{R}}{\partial \underline{\lambda}} = -\frac{\partial J}{\partial \underline{\lambda}}^\top \implies \frac{dJ}{d\underline{\eta}}^\top = \frac{dL}{d\underline{\eta}}^\top = \frac{\partial J}{\partial \underline{\eta}}^\top + \tilde{\underline{\lambda}}^\top \frac{\partial \underline{R}}{\partial \underline{\eta}} \quad . \tag{4}$$

The optimization process using the adjoint technique can be summarized as:
(1) Primal, $\underline{\lambda}$: Obtain the state variables by solving the n primal problems (for n scenarios),
(2) Adjoint, $\tilde{\underline{\lambda}}$: Obtain the adjoint variables by solving the n adjoint problems (for n scenarios),
(3) Gradient, $\underline{J}_{,\eta}$: The n gradient vectors for each of the n load cases are computed,
(4) Aggregate & Smoothen, $\underline{J}_{,\eta}^{smooth}$: Aggregate the n gradient vectors and smoothen, and
(5) Update, $\underline{\eta}_{new} = \underline{\eta}_{old} - \alpha \cdot \underline{J}_{,\eta}^{smooth}$: The parameter update is computed based on the step size α.

3 NUMERICAL STUDY

This section presents the sensitivities ($dJ/d\underline{\eta}$) for two numerical examples, namely a Flow around a Cylinder and a CAARC 2D example. In both examples, a target inlet velocity profile is defined, and a steady-state incompressible RANS (with $k-\omega-SST$ turbulence model with wall functions) solution is obtained. The velocity and pressure at the sensor locations are interpolated and set as measured data. The models are then simulated with the initial guess of inlet velocities, and the computed data at the sensors are obtained, which are used for J in Eq. (1). For the gradient calculation, the adjoint variables are obtained by solving Eq. (4), and the final gradients are computed

(a) Velocity (left) & Pressure (right) fields of the target solution and location of the 8 velocity and pressure sensors.

(b) Inlet velocity gradient (on left edge: 14 nodes) for the unsmoothed (left) and smoothed (right) cases.

Figure 1: Flow Around a Cylinder. Target Velocity: Uniform 25 m/s ($Re \approx 14,000$) on the left edge; Initial guess (for the gradients shown): Uniform 1 m/s on the left edge.

(a) Velocity (left) & Pressure (right) fields of the target solution and location of the 33 velocity and pressure sensors.

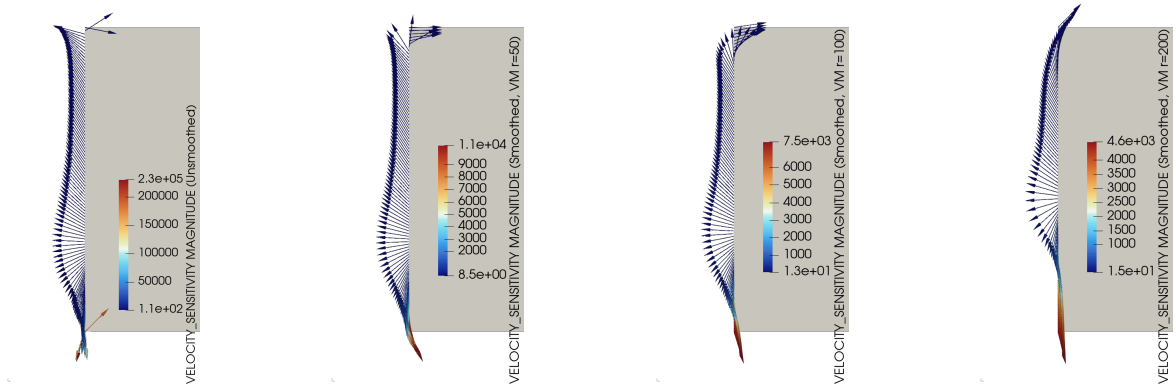

(b) Inlet velocity gradient (on left edge: 110 nodes) for the unsmoothed and smoothed cases with different VM radii.

Figure 2: CAARC 2D Example. Target Velocity: Atmospheric Boundary Layer (ABL) $25 * (y/180.0)^{0.12}$ m/s ($Re \approx 250 \cdot 10^6$) on the left edge; Initial guess (for the gradients shown): ABL $10 * (y/180.0)^{0.12}$ m/s on the left edge.

by postprocessing the adjoint variables and the partial sensitivities. To address the ill-conditioned identification problem, Vertex Morphing (VM) is employed for gradient smoothing (Hojjat et al. 2014). The target flow fields and the unsmoothed and smoothed gradients for both examples are shown in Figures 1 and 2.

4 RESULTS AND CONCLUSION

The sensitivity fields presented in Section 3 for the Flow around a cylinder and the CAARC examples show that gradients exist for the given cost function w.r.t. the considered design parameters (here, inlet velocity), and thus, can be used in an optimization loop to identify the inlet velocities. The gradients, in general, appear to point in the right direction (an arrow towards the left implies the search direction is towards the right, hence increasing the velocity guess towards the target). The ill-conditioning challenge is also evident from Figure 2, where the gradients near the bottom end vary significantly from those of the majority of the inner nodes, which could be stemming from the wall functions used. This may cause the optimizer to become stuck in a local minimum. Even the degree of regularization (influenced by the radius for vertex morphing) can alter the gradient field (cf. Figure 2b).

This explorative work is a first step in an adjoint-based optimization-driven methodology for boundary (inlet velocity profile) parameter identification for reconstructing flow fields for structures under wind flow. Naturally, we anticipate challenges to arise in this domain, such as ill-conditioning and multimodality of the identification problem, the effect of the regularization technique, and the effect of the optimization algorithm on identification accuracy.

ACKNOWLEDGEMENTS

Funded by SIEMENS AG and the Technical University of Munich, Institute for Advanced Study. The GMU team is also partially supported by the ONR N00014-24-1-2147, NSF DMS-2408877, AFOSR FA9550-25-1-0231. We also acknowledge funding by the DFG, under EXC 2163/1 - Project-ID 390881007.

REFERENCES

T. S. A. Ansari, R. Löhner, R. Wüchner, H. Antil, S. Warnakulasuriya, I. Antonau, and F. Airaudo. Adjoint-based recovery of thermal fields from displacement or strain measurements. *Computer Methods in Applied Mechanics and Engineering*, 438:117818, 2025a. doi:https://doi.org/10.1016/j.cma.2025.117818.

T. S. A. Ansari, S. Warnakulasuriya, R. Wüchner, K-U. Bletzinger, I. Antonau, R. Löhner, H. Antil, and F. Airaudo. Adjoint-based system identification for model validation and qualification. In *Engineering Materials, Structures, Systems and Methods for a More Sustainable Future*, pages 1392–1397. CRC Press, 2025b.

M. Hojjat, E. Stavropoulou, and K-U. Bletzinger. The vertex morphing method for node-based shape optimization. *Computer Methods in Applied Mechanics and Engineering*, 268:494–513, 2014.

R. Löhner, F. Airaudo, H. Antil, R. Wüchner, F. Meister, and S. Warnakulasuriya. High-fidelity digital twins: Detecting and localizing weaknesses in structures. In *AIAA SCITECH 2024 Forum*, page 2621, 2024. doi:https://doi.org/10.2514/6.2024-2621.

F. Menter. Zonal two equation kw turbulence models for aerodynamic flows. In *23rd fluid dynamics, plasmadynamics, and lasers conference*, page 2906, 1993.

S. Warnakulasuriya. *Development of Methods for Finite Element-Based Sensitivity Analysis and Goal-Directed Mesh Refinement Using the Adjoint Approach for Steady and Transient Flows*. PhD thesis, Technische Universität München, 2022. URL https://mediatum.ub.tum.de/1637721.